Int. J. Electrochem. Sci., 8 **(2013)** 11492 - 11501

International Journal of
ELECTROCHEMICAL
SCIENCE
www.electrochemsci.org

Electrospun CdTe NPs Doping Poly(phenylene vinylene) Composite Nanofibers and Their Optoelectronic Properties

Zhiyao Sun[1], *Yang Xie*[2], *Cheng Wang*[1,3,*], *Liguo Sun*[1], *Shuhong Wang*[1], *Liang Ni*[1], *Pengfei Yan*[1,*], *Yang Gao*[1], *Linlin Zang* [1], *Disi Lu* [1], *Guoqiang Xu*[1]

[1] Key Laboratory of Functional Inorganic Material Chemistry (Heilongjiang University), Ministry of Education, 150080, P.R. China
[2] Institute of Advanced Technology of Heilongjiang Academy of Science, Harbin, 150020, P.R. China
[3] Key Laboratory of Polymer Functional Materials, School of Chemical Engineering and Material, Heilongjiang University, Harbin, 150080, P.R. China
[*]E-mail: wangc_93@yahoo.com

Received: 22 June 2013 / *Accepted:* 20 July 2013 / *Published:* 20 August 2013

CdTe nanoparticles (NPs) with excellent fluorescence properties have been incorporated into poly(phenylene vinylene) precursor/polyvinyl alcohol (PPV/PVA) nanofibers by electrospinning. By using PVA as an intermediate, CdTe Nps were well dispersed inside the nanofibers when their content was moderate. The photoluminescence (PL) peak of the CdTe NPs in the as-prepared composite nanofibers was shifted from 577 nm to 566 nm comparing with CdTe in solution. This blue shift of the PL peak resulted from the different quantum confinement effects, which was caused by the different environment surrounding the CdTe NPs. The hybrid nanofibers were characterized morphologically and optically by scanning electron microscopy (SEM), transmission electron microscopy (TEM) and PL measurements.

Keywords: Nanofiber; Electrospinning; CdTe; PPV; Nanomaterials

1. INTRODUCTION

One-dimensional (1D) nanostructures, such as various nanorods, nanotubes, nanowires and nanofibers, have emerged as a powerful class of building blocks to construct nanoscaled photonic and electronic devices in recent years [1-2]. Electrospinning is one of the effective and versatile methods for the fabrication of 1D polymer nanofibers with diameters ranging from a few nanometers to several micrometers.

Organic/inorganic hybrid nanostructures have attracted increasing attention in the fabrication of various devices [3]. Especially, hybrid systems composed of polymer nanofibers involving inorganic

NPs have been considered as available nanostructures for the next generation devices. The incorporation of functional inorganic materials into polymer fibers is expected as smart materials because polymer nanofibers can be fabricated to multi-functional wearable devices. Many interrelated research have been investigated, such as PPV/TiO_2 [4], PAN/Ag [5], PVA/SiO_2 [6], PVA/Fe_3O_4 [7], and so on. Among the polymers, the conjugated polymers have potential applications in optical and electronic micromation because of their novel conductive and light-emitting properties [8, 9]. Combining conjugated polymer with aqueous synthetic NPs with low cost and toxicity was very attractive to prepare nanofibers.

In our investigation, we screened the precursory PPV having the advantages of water solubility and easy processability as the assembling building blocks. And we chose PVA as an intermediate, because the existence of PVA can increase the compatibility between CdTe NPs and PPV precursor, and avoided serious deposition of the NPs. By using the electrospinning method, we fabricated PPV precursor/PVA/CdTe composite nanofibers successfully. The composite nanofibers with excellent fluorescent and electricity properties are potentially interesting for many applications such as micro- and nano- optoelectronic devices and systems.

2. EXPERIMENTAL

2.1 Materials

Tetrahydrothiophene and p-xylylene dichloride were purchased from Tokyo Chemical Industry Co. Ltd. PVA(Dp=1750) was purchased from Acros Co. Ltd. Sodium borohydride ($NaBH_4$), tellurium (Te) powder, cadmium chloride ($CdCl_2 \cdot 2.5H_2O$) and thioglycolic acid (TGA) were all obtained from Sinopharm Chemical Reagent Co. Ltd. All the chemicals were used without further purification.

2.2 Synthesis of Thiol-stabilized CdTe NPs

Thiol-stabilized CdTe NPs were synthesized according to Ref. 10. In brief, 1.8 g $NaBH_4$ was mixed with 2.5 g Te powder in a 50 mL flask deaerated with N_2 in advance. Then 30 mL of deionized water was added into the system. The reacting system was kept in ice for about 10 h. As a result, NaHTe was obtained in clear supernatant.

At the same time, 0.4565 g $CdCl_2 \cdot 2.5H_2O$ and 0.3085 mL TGA were dissolved in 500 mL deionized water at a 1000 mL three-necked flask under strong stirring. The pH value of above solution was adjusted to 11 via 0.5 mol/L NaOH. Then, the system was deaerated by N_2 for 30 min. Finally, 0.5 mL freshly prepared NaHTe solution was transferred to the mixed solution, which was refluxed under stirring vigorously to form thiol-stabilized CdTe NPs. The obtained CdTe NPs were precipitated by an equivalent volume of acetone and washed repeatedly with deionized water.

2.3 Preparation of PPV Precursor

The PPV precursor was prepared according to Wessling's synthetic route [11] and the optimized conditions provided by Halliday and co-workers [12]. PPV precursor aqueous solution was dialyzed in water for a week, and then it was placed in a ventilated place for a week to remove the water fully. As a result, the thick solution of PPV precursor was obtained.

2.4 Preparation of Electrospinning Solutions

0.2 g PVA was dissolved in 1.8 g water to form 10% PVA solution. Then a determined amount of PPV precursor solution (the concentration of the solution was about 3 wt %) was added to the PVA solution. The mixture was stirred for 10 min, and then CdTe NPs were added into the mixture. After stirring for a while, the solution became homogenous and it was ultrasonically treated for 10 min before electrospinning. The content of CdTe NPs was 4 wt% in PVA, and 2 wt%, 3 wt%, 4 wt% and 6 wt% in PPV precursor/PVA solution, respectively. The concentration of PPV precursor in all the samples was 0.5 wt%.

2.5 Preparation of Electrospinning Nanofibers

The electrospinning setup used in this study consisted of a 10 mL syringe with a needle (IDZ 0.8 mm), an aluminum collecting plate and a high voltage supply. The PPV/PVA/CdTe spinning solutions were electrospun at a positive voltage of 20 kV and a working distance of 20 cm (the distance between the needle tip and the take-over).

2.6 Characterization

The morphology of the resulting composite nanofibers was studied by field-emission scanning electron microscopy (FE-SEM, MX2600FE) and transmission electron microscope (TEM, FEI TECNAI F20). FT-IR spectra were recorded from a KBr window on a Nicolet Avatar 360 FT-IR spectrophotometer. A combined stead state fluorescence and phosphorescence lifetime spectrometer (FLSP920) was used to obtain the PL spectra of the as-spun nanofibers and the excitation wavelength was 470 nm. The fluorescent images of the nanofibers were taken from a fluorescence microscopy (TE2000-U). X-ray diffraction (XRD) (D8 advance) studies were performed to investigate the crystallization of CdTe NPs.

3. RESULTS AND DISCUSSION

3.1 CdTe NPs Analysis

Figure 1 showed the TEM image of the synthesized CdTe NPs. As can be seen, CdTe had a good dispersed crystalline structure and the shape of the as-prepared NPs was irregular. The fringe spacing of 0.22 nm corresponded to the (220) cubical zinc blende interplanar [13].

Figure 2 showed the XRD patterns of CdTe nanocrystalline. Broad peaks typically due to the small particle size were observed, which was well in agreement with Ref. 14. The diffraction peaks of CdTe NPs can be assigned to the diffraction planes of the cubic zinc blend structure of bulk CdTe crystal. In addition, it was also clearly observed that the diffraction peaks of CdTe exhibited slight movement compared with the standard diffraction index.

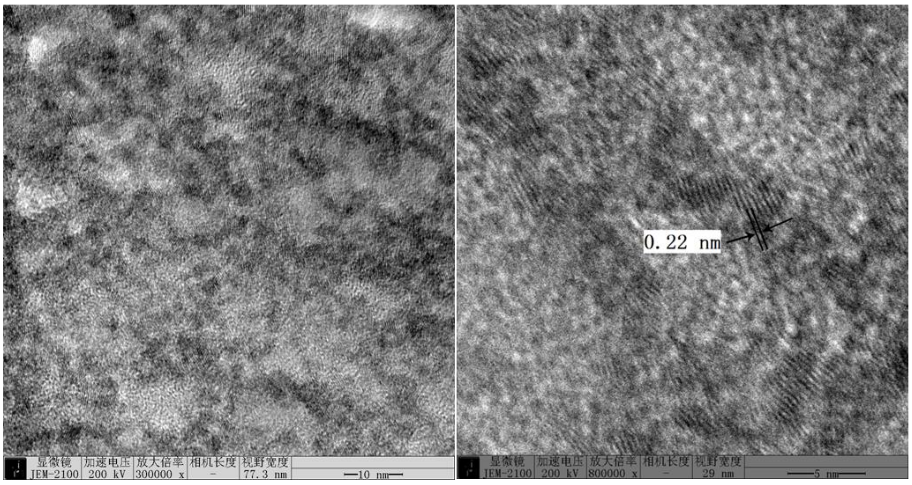

Figure 1. TEM image of CdTe NPs.

This may be due to the fact that the synthesized CdTe NPs were thiol-stabilized under the pH value of 11. Under this situation, thiol may coordinate with Cd^{2+}, and Cd-S-R complexes analogous to a shell around were formed. The existence of organics may impact the crystallization of CdTe NPs appreciably.

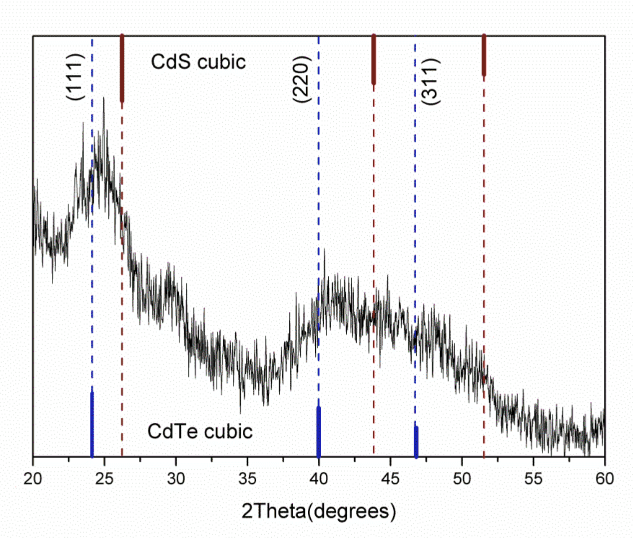

Figure 2. XRD patterns of CdTe NPs powder.

Figure 3 was the fluorescence spectrum of CdTe aqueous solution. It was clearly seen that CdTe had a main emission peak at 577 nm, which was consistent with the bright orange observed from the photo (insert of Figure 3).

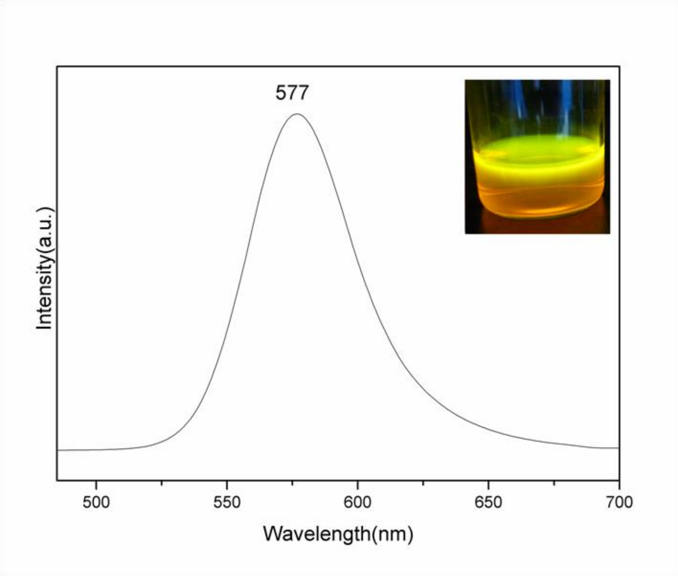

Figure 3. Fluorescence spectrum of CdTe aqueous solution (insert part is the photo of CdTe under the illumination of UV-light).

3.2 PPV/PVA/CdTe Composite Nanofibers Analysis

3.2.1 Morphology Analysis

Figure 4 presented the FE-SEM images of the electrospun nanofibers. All the nanofibers with smooth surface were randomly oriented. Pure PVA nanofibers were homogeneous and continuous with an average diameter of 276 nm (Figure 4a). After the introduction of CdTe NPs, the average diameter of PVA nanofibers decreased to 235 nm (Figure 4b). The SEM images of PPV precursor/PVA/CdTe nanofibers were shown in Figure 4c-4f. The addition of PPV precursor in the nanofibers had an important effect on the diameter of the composite nanofibers (the diameter decreased from 235 nm to 198 nm). This phenomenon can be explained that the addition of PPV precursor and CdTe NPs increased the electric conductivity of the electrospinning solution. High conductivity resulted in sufficient elongation of a jet by electrical force, consequently produced thinner nanofibers [15].

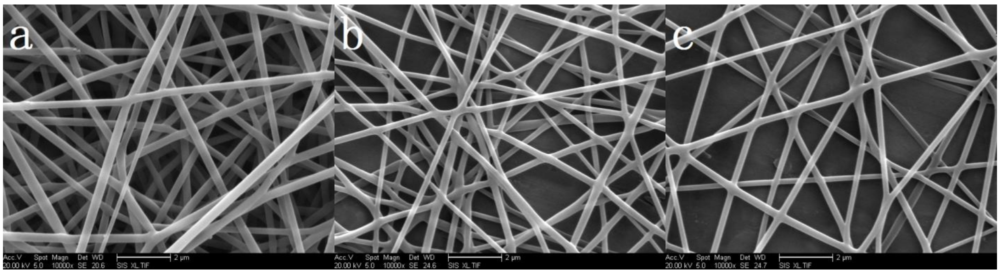

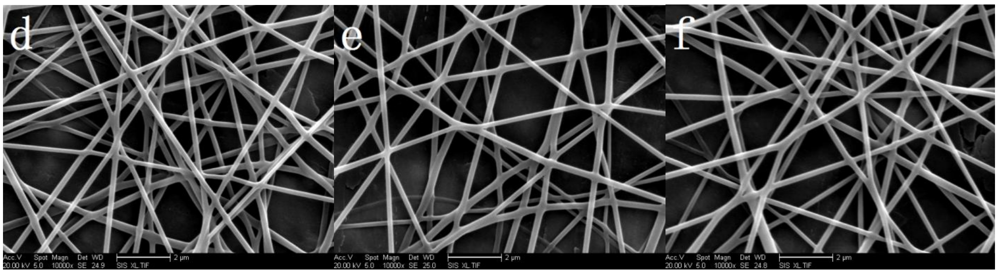

Figure 4. SEM images of the nanofibers: (a) PVA, (b) PVA/CdTe(4 wt%), (c) PPV precursor/PVA/CdTe (2 wt%), (d) PPV precursor/PVA/CdTe(3 wt%), (e) PPV precursor/PVA/CdTe(4 wt%) and (f) PPV precursor/PVA/CdTe(6 wt%).

The internal morphology and the CdTe NPs dispersion of the composites were investigated by TEM, presented in Figure 5. It can be clearly seen that the CdTe NPs were basically uniformly dispersed in the PVA nanofibers and their average diameter was only a few nanometers (Figure 5a). Owing to the exchange of the electric charges, the dispersion of CdTe NPs was somewhat affected when PPV precursor was inducing into the nanofibers. Some of the NPs began to aggregate with the increase of the content of CdTe. When the content of CdTe NPs reached to 6 wt%, the NPs formed large aggregation. Consequently, the existence of PVA weakened the interaction between the NPs and the PPV precursor, and the NPs were basically uniformly dispersed in the composite nanofibers when their concentration was moderate.

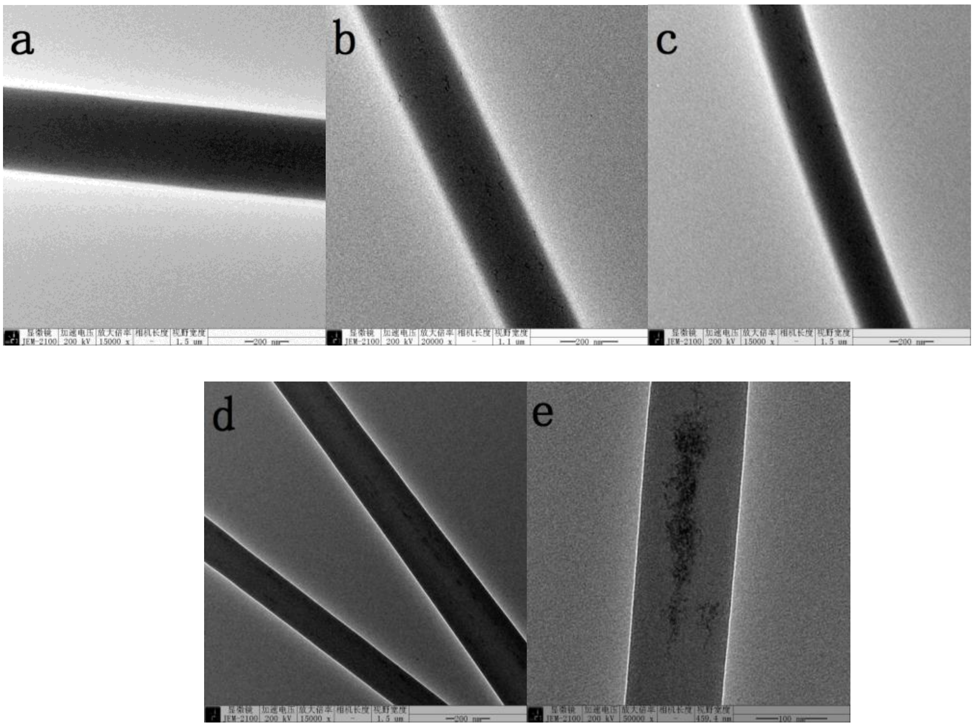

Figure 5. TEM images of the as-prepared nanofibers: (a) PVA/CdTe(4 wt%), (b) PPV precursor/PVA/CdTe(2 wt%), (c) PPV precursor/PVA/CdTe(3 wt%), (d) PPV precursor /PVA/CdTe(4 wt%) and (e) PPV precursor/PVA/CdTe(6 wt%).

3.2.2 FT-IR Spectra Analysis.

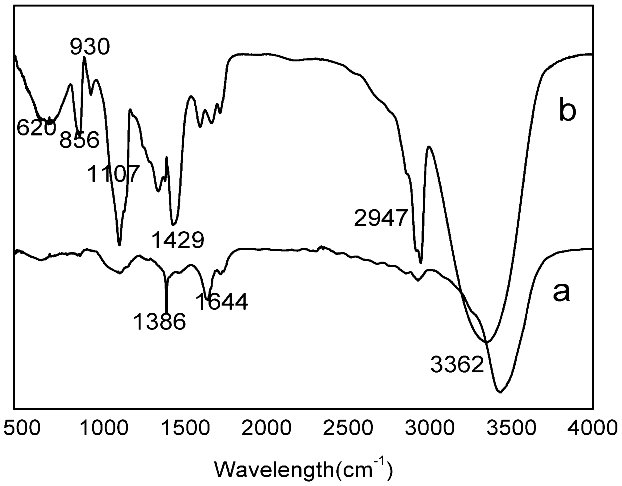

Figure 6. FT-IR spectra of the nanofibers: (a) PVA/CdTe and (b) PPV precursor/PVA/CdTe.

Figure 6 presented the FT-IR spectra of the nanofibers in the wavenumber ranging from 500 to 4000 cm^{-1}. For the PVA/CdTe nanofibers, the absorption peaks at 1386 cm^{-1} and 1644 cm^{-1} were due to C=C stretching vibration; the absorption peak at 2947 cm^{-1} was assigned to C-H stretching vibration. Additionally, it can be found that the characteristic peak of O-H group at 3362 cm^{-1} appeared in the spectrum, which was regarded as the associated hydrogen bonds among the molecules. Different from Figure 6a, there were some obvious absorption peaks belonging to PPV precursor in Figure 6b. The peaks at 620 cm^{-1}, 852 cm^{-1} and 930 cm^{-1} were due to C-S stretching vibration, C-H plane bending vibration of p-substituted of benzene ring and C-H out-of-plane vibration of trans-ethylene respectively. It was implied that the backbone structure of PPV precursor was not damaged when mixing with PVA and CdTe. However, the peak at 1107 cm^{-1} seen from Figure 6b belonged to C–O–C asymmetric stretching mode, which revealed that the PPV precursor preferred to react with PVA to form C–O–C linkages.

3.2.3 Fluorescence Spectra Analysis.

In order to study the fluorescence properties of the nanofibers, the fluorescence spectra of CdTe aqueous solution, PVA/CdTe nanofibers and PPV precursor/PVA/CdTe nanofibers were conducted when the excitation wavelength was 470 nm. Figure 7a showed the PL spectrum of the PVA/CdTe nanofibers and a main emission was seen at 566 nm which originated from the CdTe NPs. The blue shift of CdTe from 577 nm (CdTe aqueous solution, Figure 3) to 566 nm (PVA/CdTe nanofibers) may be resulted from the quantum confinement effects. In the drying process of polymer solutions, the evaporation rate of the solvent affected the microstructures of polymer, which brought about the changes in the physical and mechanical properties [16]. The evaporation rate of the solvent in the electrospinning process was very fast because of the enlarged surface areas. In addition, the applied electric field also accelerated the evaporation of solvent, which has been reported in the literature [17]. The difference in the quantum confinement effects depended on the microstructure wrapping around CdTe NPs-related PL peak. Namely, in the case of pure CdTe NPs solution, the CdTe NPs were surrounded by water, whereas in the CdTe composite nanofibers, the CdTe NPs were surrounded by PVA and PPV precursor molecules.

In Figure 7, the inset was the PL spectrum of PPV precursor nanofibers. It was clearly seen that the main emission was at 521 nm, which presented obvious blue shift compared with that of pure PPV(554 nm) [4]. Figure 7b-e gave the PL spectra of the PPV precursor/PVA/CdTe composite nanofibers. It can be found that a new emission at 513 nm appeared when PPV precursor existed in the composite nanofibers, which exhibited slight blue shift compared with that of PPV precursor nanofibers (521 nm). This phenomenon can be explained by two reasons: First, the PPV precursor was not further heated over 220 ℃; Second, part of the PPV precursor chain reacted with PVA to form C-O-C linkages, which interrupted the conjugation of PPV polymer chains and decreased the p-conjugated chain length [18]. When the CdTe NPs concentration increased from 2 wt% to 6 wt%, the emission peak of the CdTe NPs near 560 nm shifted from 554 nm to 561 nm as a result of light re-adsorption and/or slight Fluorescence Resonance Energy Transfer (FRET) [19]. Besides, the PL intensity of CdTe NPs was enhanced with the increase of CdTe concentration. The PL results indicated that the NPs dispersed well in the resulting nanofibers and the process of electrospinning prevented the further occurrence of FRET.

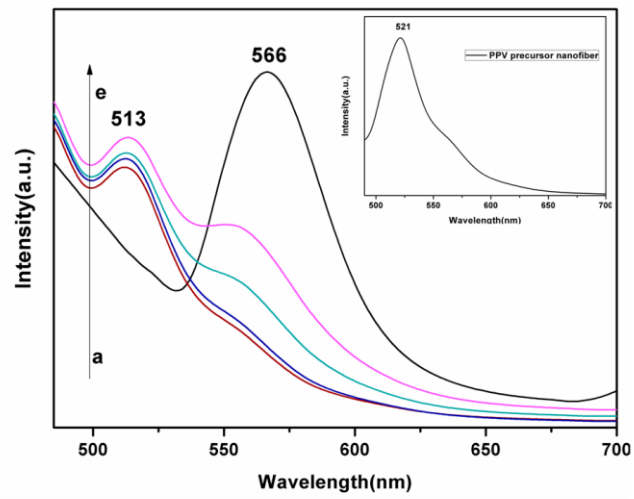

Figure 7. Fluorescence spectra of the composite nanofibers: (a) PVA/CdTe(4 wt%), (b) PPV precursor/ PVA/CdTe(2 wt%), (c) PPV precursor/PVA/CdTe(3 wt%), (d) PPV precursor/PVA/CdTe(4 wt%) and (e) PPV precursor/PVA/CdTe(6 wt%). Inset is the fluorescence spectrum of PPV precursor nanofibers.

3.2.4 Fluorescence Photos Analysis.

Figure 8 showed the fluorescence photos of the composite nanofibers. It was clearly seen that all the nanofibers were disordered and they were more than several millimeters in length, which was in accordance with the results of the SEM images. PVA matrix was non-luminous and pellucid, thus the orange CdTe NPs inside the nanofibers can be clearly seen. And the NPs were well dispersed in the composite fibers. When introducing PPV precursor, the color of the nanofibers turned from orange to yellow-green which originated from the PPV structure. Although the content of PPV precursor was low, the fluorescence intensity was still strong. When the content of CdTe NPs was less than 4 wt%, the NPs were hardly seen from the photos. In Figure 8d and 8e, some aggregated particles can be observed clearly, and the fluorescence color of nanofibers had slightly changed.

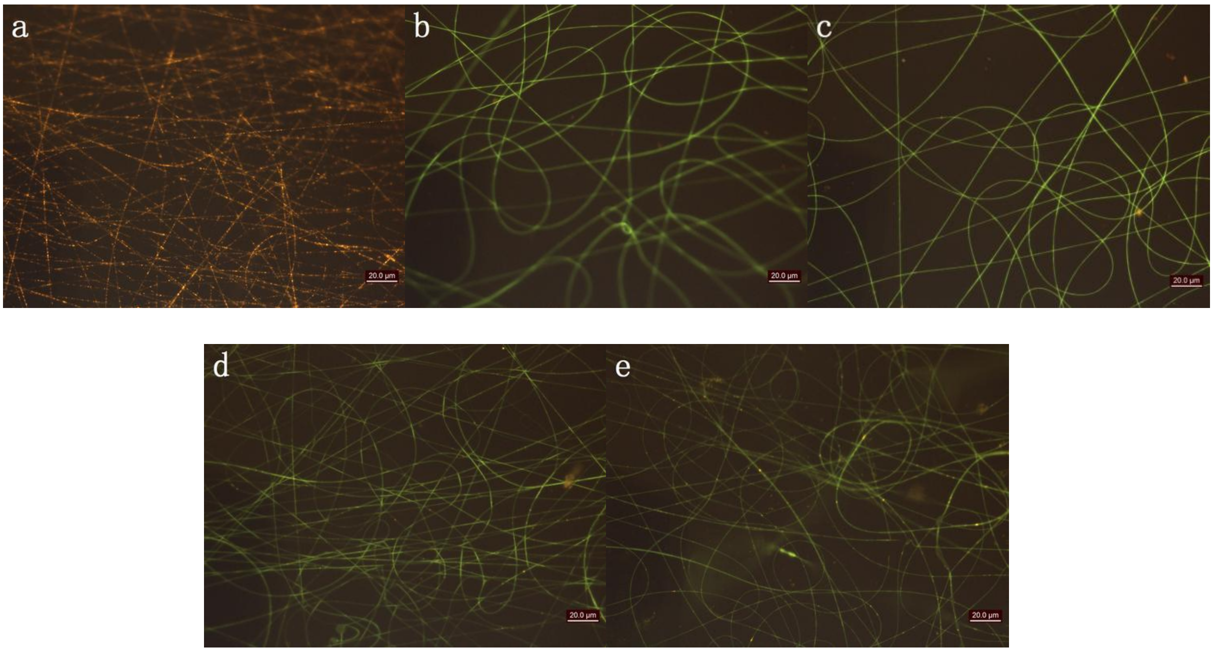

Figure 8. The fluorescence photos of composite nanofibers: (a) PVA/CdTe(4 wt%), (b) PPV precursor/PVA/CdTe(2 wt%), (c) PPV precursor/PVA/CdTe(3 wt%), (d) PPV precursor/ PVA/CdTe(4 wt%) and (e) PPV precursor/PVA/CdTe(6 wt%).

4. CONCLUSIONS

The thiol-stabilized CdTe NPs with excellent fluorescence properties were synthesized successfully. By using PVA as an intermediate, the PPV precursor/PVA/CdTe composite nanofibers were fabricated by electrospinning. The SEM results showed that the composite nanofibers were homogeneous and continuous and the addition of PPV precursor and CdTe NPs had an important effect on the diameter of the composite fibers. FT-IR spectra showed clearly that the PPV precursor preferred to react with PVA to form C–O–C linkages which may result in the blue shift of the PL spectrum of PPV. The PL peak of the CdTe NPs in the composite nanofibers was shifted from 577 to 566 nm, which indicated that the existence of quantum confinement effects tied to the quantum structures. This information may be useful for the further preparation of CdTe NPs embedded nanofibers.

ACKNOWLEDGMENT
The present study has been supported by NSFC (51273056, 21202091, 21074031 and 51310105037), CPDF (201104456), NSF of Heilongjiang (E201118 and E201144), Abroad Person with Ability Foundation of Heilongjiang Province (2010Td03 and 12521400) and Innovation Fellowship Foundation of Heilongjiang University (Hdtd2010-11).

References

1. N.K. Hassan, M.R. Hashim, Y. Al-Douri and K. Al-Heuseen, *Int. J. Electrochem. Sci.*, 7 (2012) 4625.
2. Y. Xia, P. Yang, Y. Sun, Y. Wu, B. Mayers, B. Gates, Y. Yin, F. Kim and H. Yan, *Adv. Mater.*, 15 (2003) 353.
3. J. Bouclé, P. Ravirajan and J. Nelson, *J. Mater. Chem.*, 17 (2007) 3141.
4. C. Wang, E.Y. Yan, Z.H. Huang, Q. Zhao and Y. Xin, *Macromol. Rapid Commun.*, 28 (2007) 205.
5. Q.B. Yang, D.M. Li, Y.L. Hong, Z.Y. Li, C. Wang, S.L. Qiu and Y. Wei, *Synthetic Met.*, 137 (2003) 973.
6. M Krissanasaeranee, T. Vongsetskul, R. Rangkupan, P. Supaphol and S. Wongkasemjit, *J. Am. Ceram. Soc.*, 91 (2008) 2830.
7. S.H. Wang; C. Wang, B. Zhang, Z.Y. Sun, Z.Y. Li, X.K. Jiang and X.D. Bai, *Mater. Lett.*, 64 (2010) 9.
8. Z. Wen, E. Yan and Z. Huang, *Curr. Appl. Phys.*, 9 (2009) 189.
9. N. Hamizi, C. Ying and M. Johan, *Int. J. Electrochem. Sci.*, 7 (2012) 4727.
10. H. Zhang, Z. Zhou, B. Yang and M.Y. Gao, *J. Phys. Chem. B*, 107 (2003) 8.
11. R.A. Wessling, *J. Polym. Sci: Polym. Symp.*, 72 (1985) 55.
12. D.A.D. Halliday, P.L. Burn, R.H. Friend, D.D.C. Bradley and A.B. Holme, *Synthetic Met.*, 55 (1993) 902.
13. C. Wu, L. Shi, Q. Li, H. Jiang, M. Selke, L. Ba and X. Wang, *Chem. Res. Toxicol.*, 23 (2010) 82.
14. H. Zhang, Z. Zhou and B.J. Yang, *J. Phys. Chem. B*, 107 (2003) 8.
15. N. Bhardwaj and S.C. Kundu, *Biotechnol. Adv.*, 28 (2010) 325.
16. R. Fernández, P. Ferreira-Aparicio and L. Daza, *J. Power. Sources.*, 151 (2005) 18.
17. F.C. Lai, M. Huang and D.S. Wong, *Drying Technol.*, 22 (2004) 597.
18. W. Zhang, Z.H. Huang, E.Y. Yan, C. Wang, Y. Xin, Q. Zhao and Y.B. Tong, *Mater. Sci. Eng. A*, 443 (2007) 292.
19. M.J. Li, J.H. Zhang, H. Zhang, Y.F. Liu, C.L. Wang, X. Xu, Y. Tang and B. Yang, *Adv. Funct. Mater.*, 17 (2007) 3650.